An intercomparison of tropospheric ozone retrievals derived from two Aura instruments and measurements in western North America in 2006

D. C. Doughty,[1] A. M. Thompson,[1] M. R. Schoeberl,[2] I. Stajner,[3] K. Wargan,[4,5] and W. C. J. Hui[1,6]

Received 30 June 2010; revised 3 December 2010; accepted 4 January 2011; published 17 March 2011.

[1] Two recently developed methods for quantifying tropospheric ozone abundances based on Aura data, the Trajectory-enhanced Tropospheric Ozone Residual (TTOR) and an assimilation of Aura data into Goddard Earth Observing System Version 4 (ASM), are compared to ozone measurements from ozonesonde data collected in April–May 2006 during the INTEX Ozonesonde Network Study 2006 (IONS-06) campaign. Both techniques use Ozone Monitoring Instrument (OMI) and Microwave Limb Sounder (MLS) observations. Statistics on column ozone amounts for both products are presented. In general, the assimilation compares better to sonde integrated ozone to 200 hPa (28.6% difference for TTOR versus 2.7% difference for ASM), and both products are biased low. To better characterize the performance of ASM, ozone profiles based on the assimilation are compared to those from ozonesondes. We noted slight negative biases in the lower troposphere, and slight positive biases in the upper troposphere/lower stratosphere (UT/LS), where we observed the greatest variability. Case studies were used to further understand ASM performance. We examine one case from 17 April 2006 at Bratt's Lake, Saskatchewan, where geopotential height gradients appear to be related to an underestimation in the ASM in the UT/LS region. A second case, from 21 April 2006 at Trinidad Head, California, is a situation where the overprediction of ozone in the UT/LS region does not appear to be due to current dynamic conditions but seems to be related to uncertainty in the flow pattern and large differences in MLS observations upstream.

Citation: Doughty, D. C., A. M. Thompson, M. R. Schoeberl, I. Stajner, K. Wargan, and W. C. J. Hui (2011), An intercomparison of tropospheric ozone retrievals derived from two Aura instruments and measurements in western North America in 2006, *J. Geophys. Res.*, *116*, D06303, doi:10.1029/2010JD014703.

1. Introduction

[2] Tropospheric ozone is an important trace gas because it has deleterious effects on human health and agriculture [*Fares et al.*, 2010], and because of its role in climate change [*Intergovernmental Panel on Climate Change*, 2007]. For these reasons, it is important to be able to measure global distributions of tropospheric ozone. From the time of the earliest estimates of tropospheric ozone from space [*Fishman et al.*, 1990] to the present day, the need to follow continental and intercontinental-scale pollution, which includes ozone, has required greater resolution and higher accuracy satellite data. The Earth Observing System (EOS) constellation of satellites, Terra, Aqua, and Aura, have contributed in many ways to global sampling of gaseous and particulate pollution [*Yu et al.*, 2010; *Park et al.*, 2007]. Nonetheless, tropospheric ozone retrievals remain a challenge for which a variety of approaches have been developed in the past 10 years.

[3] The tropospheric ozone residual (TOR) pioneered these techniques, subtracting Stratospheric Aerosols and Gases (SAGE) retrievals of stratospheric column ozone from Total Ozone Mapping Spectrometer (TOMS) total column ozone (TCO) in order to retrieve tropospheric ozone values [*Fishman et al.*, 1990]. This technique only offered seasonal mean values. To extend this method to higher time resolutions, there exist several options. Combination of different data sets can be used, such as potential vorticity mapping for global coverage [*Yang et al.*, 2010], or improving the handling of cloudy conditions [*Ziemke et al.*, 2006]. Additional methods involve the use of mathematical techniques to invert top-of-atmosphere radiance measurements to retrieve ozone profiles [*Liu et al.*, 2010].

[4] *Zhang et al.* [2010] uses several different methods to intercompare tropospheric ozone profiles from the Tropo-

[1]Department of Meteorology, Pennsylvania State University, University Park, Pennsylvania, USA.
[2]Science and Technology Corporation, Hampton, Virginia, USA.
[3]Noblis, Inc., Falls Church, Virginia, USA.
[4]Global Modeling and Assimilation Office, NASA Goddard Space Flight Center, Greenbelt, Maryland, USA.
[5]Science Applications International Corporation, Beltsville, Maryland, USA.
[6]Trinity Consultants, Dallas, Texas, USA.

0148-0227/11/2010JD014703

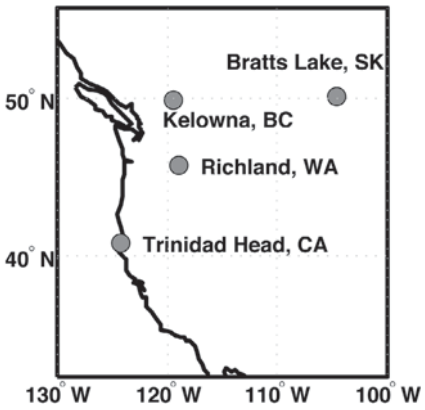

Figure 1. IONS-06 western United States/Canada ozonesonde launch sites in 2006.

spheric Emission Spectrometer (TES) and the Ozone Monitoring Instrument (OMI) with in situ ozonesondes. The present study compares two different retrieval methods which use the same satellite data, total ozone column retrievals from OMI, and stratospheric ozone profiles from the Microwave Limb Sounder (MLS), two instruments on board NASA's Aura satellite. The methods compared are a residual method by *Schoeberl et al.* [2007], the Trajectory-Enhanced Tropospheric Ozone Residual (TTOR), and an assimilation-model-derived product [*Stajner et al.*, 2008] based on the Goddard Earth Observing System (GEOS, version 4).

[5] Aura-derived tropospheric ozone and ozone profiles from these products are compared with measurements from ozonesondes launched during the April–May 2006 INTEX-B (Intercontinental Transport Experiment-Phase B)/IONS-06 (INTEX Ozonesonde Network Study, 2006) campaign [*Thompson et al.*, 2008]. One of the main objectives of the INTEX-B campaign was to validate measurements from the Aura satellite from aircraft and ground-based sites in North America, with the April–May period focusing on trans-Pacific transport of pollutants [*Singh et al.*, 2009; *Zhang et al.*, 2009]. The IONS sites we examine here are Bratt's Lake, Saskatchewan; Kelowna, British Columbia; Richland, Washington; and Trinidad Head, California (Figure 1).

2. Methods

[6] We compare two different tropospheric ozone products that use data from the Aura satellite with in situ measurements made by ozonesondes. The first step in this analysis is to examine integrated ozone from the surface to 200 hPa (an approximation of tropopause height). Then, we look at impacts that satellite retrieval errors may have on the tropospheric ozone estimation, and consider ozone profiles from the assimilation. Finally, we conduct case studies to improve understanding of factors that lead to better or worse comparisons between sondes and satellite products.

2.1. Data Products

2.1.1. Aura Instruments

[7] Aura orbits at a height of 705 km, with an orbital period of 98.8 min. It is a Sun-synchronous, polar-orbiting satellite, crossing the equator at 1345 local time on its ascending node [*Levelt et al.*, 2006; *Waters et al.*, 2006]. The Ozone Monitoring Instrument (OMI) was designed to measure ozone and other trace gases, with a small footprint and daily global coverage. OMI's nadir pointing telescope has a 13 km by 28 km footprint, and swath width of each scan is 2600 km [*Levelt et al.*, 2006]. Data examined in this study use the Total Ozone Mapping Spectrometer (TOMS-v8) retrieval algorithm. On average, the OMI-TOMS (hereafter referred to as OMI) retrievals of total column ozone agree better than 1% [*McPeters et al.*, 2008; *Balis et al.*, 2007] with ground-based Brewer and Dobson spectrometers.

[8] The Microwave Limb Sounder (MLS) scans in the plane of orbital motion, retrieving individual profiles every 165 km along its track. The vertical resolution is 3 km, and approximate horizontal resolution is 300 km in the upper troposphere/lower stratosphere (UT/LS) region. Precision ranges from 20% at the 215 hPa level to 3–5% in the stratosphere [*Froidevaux et al.*, 2008; *Boyd et al.*, 2007]. Of the methods described in Table 1, we consider two products that use data from OMI and MLS.

2.1.2. Aura-Derived Troposphere Products

[9] The first product examined is the Trajectory-enhanced Tropospheric Ozone Residual (TTOR). The version (1.6) of the TTOR product used in this study uses 2-day isentropic backward and forward trajectories from GEOS-4 [*Bloom et al.*, 2005] to map MLS measurements over the Earth's surface, followed by interpolation of these values to a 1.25° × 1° grid. This differs from the version described by *Schoeberl et al.* [2007], which used 6 day isentropic forward trajectories. Stratospheric column ozone is calculated from the mapped and interpolated MLS measurements, and then is subtracted from interpolated OMI total column ozone. The results of this calculation are daily global estimates of tropospheric ozone.

[10] The Aura assimilation, hereafter referred to as ASM, is described in detail by *Stajner et al.* [2008], and we only give a brief summary here. The ASM combines MLS stratospheric ozone profiles (216–0.14 hPa) and OMI total ozone with 3 h ozone forecasts generated by the GEOS-4

Table 1. Several Methods to Retrieve Tropospheric Ozone Column From Satellite Data

Technique	Principles Involved	Reference
Tropospheric Ozone Residual (TOR)	Subtract SAGE SCO from TOMS TCO	*Fishman et al.* [1990]
Trajectory-Enhanced TOR	TOR using trajectory-mapped MLS for global coverage	*Schoeberl et al.* [2007]
TOR with Convective Cloud Differential	Calibrate TOR with OMI CCD	*Ziemke et al.* [2006]
PV mapped TOR	TOR using PV-mapped MLS	*Yang et al.* [2007]
OMI Estimation	Optimal Estimation	*Liu et al.* [2010]
Multi-Sensor Upper Troposphere Ozone	TES ozone and GOES water vapor	*Felker et al.* [2010]
OMI/MLS assimilation into GEOS-4	GEOS-4, TCO and MLS profile	*Stajner et al.* [2008]

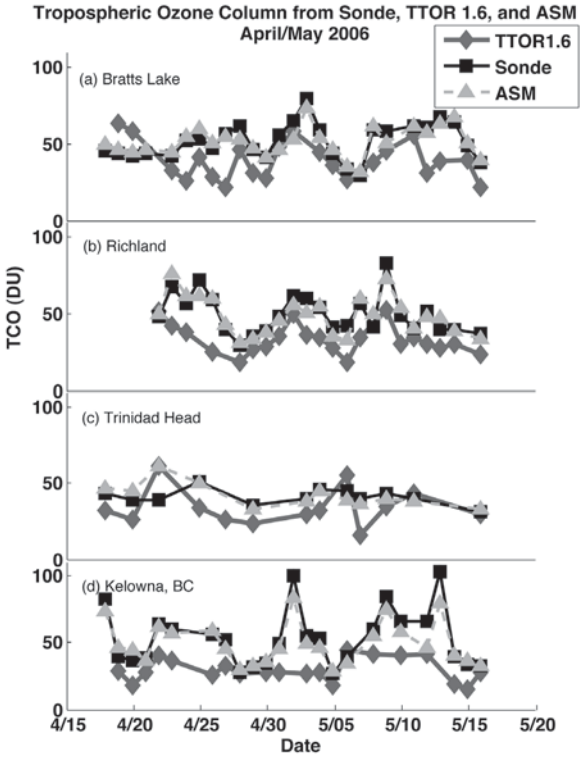

Figure 2. Time series for surface to 200 hPa integrated column ozone.

meteorological data assimilation system (DAS). The GEOS-4 DAS is as described by *Bloom et al.* [2005]; however, here the forecasts are initialized with 6 hourly averaged winds rather than instantaneous winds because *Pawson et al.* [2007] showed that transport is substantially improved if such averaging is applied. The system is run at a 1° × 1.25° spatial resolution with 55 vertical layers between the surface and 0.01 hPa. Typically, 12 of those layers lie below 200 hPa.

[11] Ozone chemistry in the assimilation is approximated by two simplified schemes. In the stratosphere, monthly zonal production (P) and loss (L) rates are applied. The P and L values are based on the work by *Douglass et al.* [1996]. The tropospheric chemistry scheme uses daily three-dimensional production, loss rates and dry deposition velocities derived from a separate run of the GEOS-Chem model (version 7.04) for the same period [*Hudman et al.*, 2007]. The ASM chemical constituent output is available at the model spatial resolution in 3 h intervals.

2.1.3. Ozonesondes and Study Location

[12] The IONS-06 ozone profiles were collected using balloon-borne electrochemical concentration cell (ECC) ozonesondes, which measure ozone partial pressure from the surface to nearly 7 hPa, and transmit these measurements back to a ground station, along with standard radiosonde measurements of pressure, temperature, and humidity [*Komhyr*, 1969]. All sites used En-Sci ECC ozonesondes, and slightly different solution buffers, but all procedures optimize accuracy in the troposphere. The precision of the ozone profile in the troposphere is 5–10% [*Smit et al.*, 2007], and varies somewhat at different levels. Elevated pump current was observed on one day, but this would not have affected measurement in the troposphere (S. Oltmans, personal communication, 2009).

[13] As a strategic campaign network [*Thompson et al.*, 2011], IONS-06 (http://croc.gsfc.nasa.gov/intexb/ions06.html) provided ozone profiles at a frequency near one launch per day, close to the Aura overpass time at sites throughout North America (Figure 1). Spring months were chosen for the present analysis because the dynamical variability as the polar jet moves northward may present a problem for some models. Thus, this regime represented a good test case for these data products.

[14] Four study sites from the IONS-06 campaign (Figure 1) are selected because they are geographically close, yet topographically diverse. Bratt's Lake, Saskatchewan [50.2° N, 104.7°W], is located at 580 meters above sea level (ASL) on the plains in southern Canada; Kelowna, British Columbia [49.9°N, 119.4°W], is located in the Cascade Mountains at 456 m ASL; Richland, Washington [46.0°N, 119.0°W], is located on the slopes of the Cascade Mountains at 123 meters above sea level (ASL); and Trinidad Head, California [40.8°N, 124.2°W], is less than a kilometer from the Pacific Ocean at 127 m ASL. Additionally, these sites had relatively more measurements during the Spring 2006 intensive period than many of the other sites.

2.2. Calculations and Analysis

2.2.1. Tropospheric Column Comparisons

[15] TTOR provides tropospheric ozone column data, but for the ASM product and the ozonesondes, we need to calculate column amounts. For ASM, ozone mixing ratios are linearly interpolated to regular levels between the surface and the tropopause, and then integrated using the equation

$$0.7891 \int_{p_t}^{p_s} \mu \cdot dp \tag{1}$$

as described by *Stajner et al.* [2008]. The result of equation (1) is ozone amount for the layer in Dobson Units (DU), or 2.69×10^{16} molecules per square centimeter. In equation (1), μ is the ozone mixing ratio in parts per million by volume (ppmv), p is the pressure, p_t is the tropopause pressure, and p_s is the surface pressure in hPa. For ozonesonde data, we applied the equation

$$26.93 \int_{z_t}^{z_s} \frac{p(z)\mu_z}{T(z)} dz, \tag{2}$$

where p(z) is the pressure at height z (meters), z_t is the tropopause height, z_s is the surface height, $T(z)$ is the temperature in degrees Kelvin, and μ_z is the ozone concentration in ppmv [*Dougherty*, 2008]. We use these methods because

Table 2. Errors (Err), Standard Deviations (Stdev), and Percent Differences (%) for TTOR and ASM

	Product					
	TTOR			ASM		
Location	Err (DU)	Stdev(DU)	%	Error (DU)	Stdev(DU)	%
Bratt's Lake	−12.5	12.7	24.1	−0.42	4.9	0.81
Kelowna	−16.7	9.7	31.4	−4.0	7.5	7.5
Trinidad Head	−6.3	12.9	−15.4	0.89	7.4	2.1
Richland	−16.4	8.7	32.9	−0.68	5.9	1.4

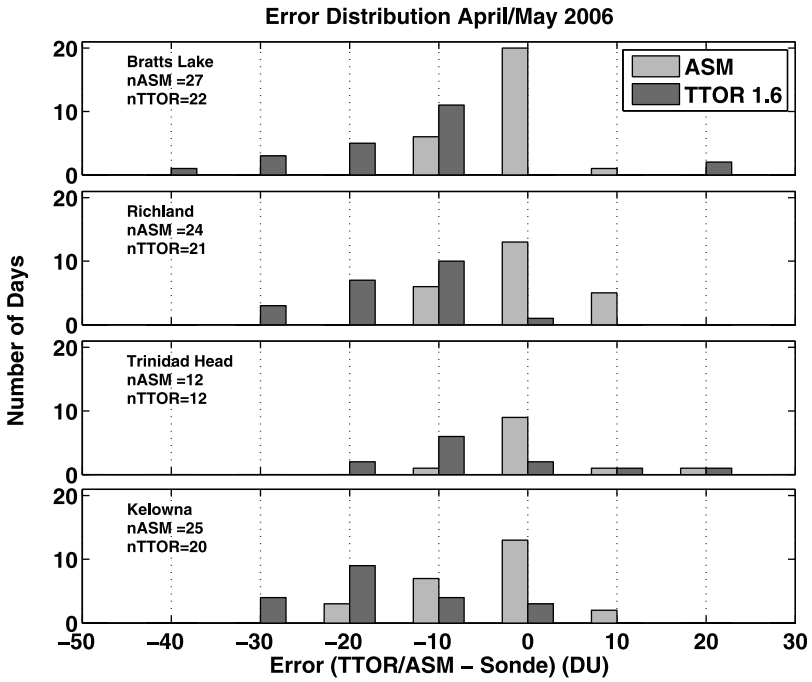

Figure 3. Histograms of surface to 200 hPa integrated column ozone errors. Bars are placed at the center of each bin, 10 DU apart.

each is standard for respective analyses. We also calculated sonde columns using equation (1), and there was little change in statistics or column amounts.

[16] A number of tropopause definitions have been employed in the calculation of tropopause column amount from sonde and satellite data, such as changes in lapse rate, differences in potential vorticity (dynamical), cold point temperature, and ozonopause [*Dougherty*, 2008]. In this study, 200 hPa is selected as the upper bound for tropospheric ozone to minimize ambiguities associated with these definitions [*Schoeberl et al.*, 2007; *Stajner et al.*, 2008]. Once column estimates are produced for the sondes and ASM, we calculate errors and percent differences for each day of the study period. We also compare the correlation of biases in OMI total ozone column (OMI - ozonesonde total), to 200 hPa tropospheric column biases (TTOR/ASM–ozonesonde troposphere) to determine if error in the OMI total column amount for a given day tends to dominate the corresponding tropospheric ozone discrepancy.

2.2.2. Profile Analysis and Case Studies

[17] ASM provides ozone mixing ratios throughout the troposphere, so we examine the performance of individual ASM profiles. We average ozonesonde measurements over the ASM product pressure levels, and then compare ASM with in situ ozonesondes.

[18] Finally, we develop case studies to understand irregularities in the performance of the ASM ozone estimation method, with the goal of determining if meteorological conditions have an impact on the accuracy of this data product. Where possible, meteorological data from the GEOS model [*Bloom et al.*, 2005] are used for analysis of the dynamic conditions because they were used for computation of trajectories in TTOR and dynamical evolution in ASM. However, these data were supplemented with NCEP fields in some cases.

3. Results

3.1. Tropospheric Ozone Column Comparison

[19] Time series comparisons of tropospheric ozone columns with TTOR and ASM are shown in Figure 2 for all four locations. Note that both the TTOR and the ASM

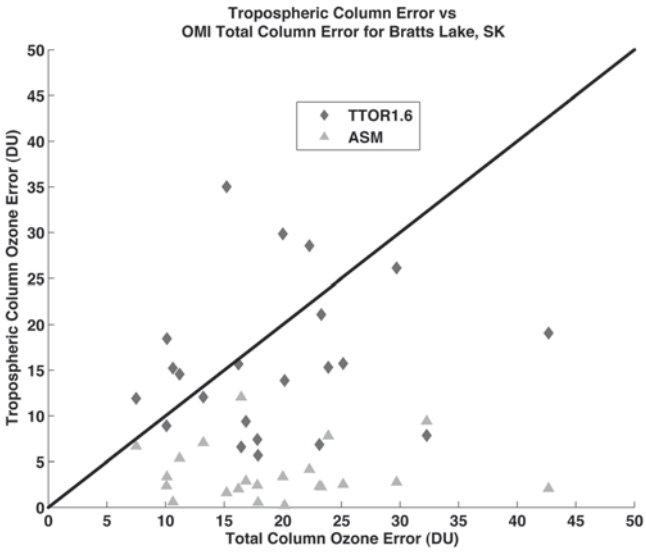

Figure 4. Absolute values of OMI total column ozone biases(OMI-sonde) versus tropospheric column ozone biases(TTOR/ASM - sonde) at Bratt's Lake, Saskatchewan.

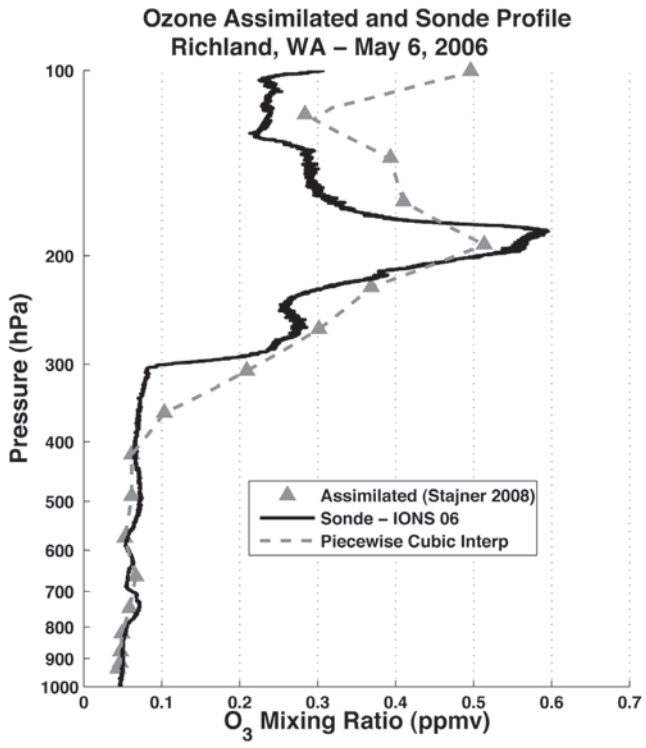

Figure 5. An example of sonde (black) and ASM (gray) profiles in the troposphere and lower stratosphere on 6 May 2006.

products capture the general patterns measured by the ozonesondes, although TTOR is biased lower than ASM when compared with sondes, consistent with work by *Schoeberl et al.* [2007]. *Yang et al.* [2010] also report a low bias in Tropospheric Column Ozone (TCO) derived from newer retrievals of OMI and MLS when compared to IONS sondes. TTOR exhibits low ozone during several high-ozone episodes in Kelowna, and some additional days with high ozonesonde tropospheric ozone column amounts were flagged in the TTOR product, and are not included in this analysis. Additionally, while both products retrieve lower tropospheric ozone column values than sondes on average, an exception occurred on 21 April at Trinidad Head, California (Figure 2b), when both TTOR and ASM significantly overpredict ozone; this case is discussed below. The mean statistics of data product biases can be seen in Table 2, where TTOR tropospheric ozone values are biased low by 13.7 DU (28.6%) on average compared with ozonesondes, and ASM column amounts are biased low by 1.3 DU (2.7%). ASM is also more correlated to the ozonesondes, with a correlation coefficient of 0.91, whereas TTOR has a correlation coefficient of 0.49. The TTOR correlations and standard deviations are similar to those reported by *Schoeberl et al.* [2007] for the March, April, and May periods from 30°N to 60°N, however average differences are quite a bit larger. Although the biases do not appear to be normally distributed, we may still retrieve some use out of the standard deviations (Table 2), noting that the standard deviation for the ASM is 6.4 DU, whereas the average standard deviation for TTOR is 11.3 DU.

[20] Histograms that offer a qualitative look at the biases for the four locations are shown in Figure 3. Distribution of errors is slightly skewed for both data products, and is slightly narrower for ASM than for TTOR. The spread of the TTOR retrieval errors, as well as computed standard deviations, are larger at Trinidad Head, California, and Bratt's Lake, Saskatchewan, than at Richland, Washington, and Kelowna, British Columbia. This result may be surprising, as one might expect the Kelowna comparisons to vary more due to dynamic complexity in the mountainous terrain (456 m ASL). Kelowna does have one of the highest percent differences for TTOR, and the highest for ASM, suggesting that there is a lot of expected variability at this site.

[21] We note that most of the ASM errors are centered about the mode at zero for all sites, whereas the TTOR errors are centered about the mode of −10 DU, except in Kelowna where the mode is −20 DU. Thus, even though the data are not normally distributed, it appears that the computed sta-

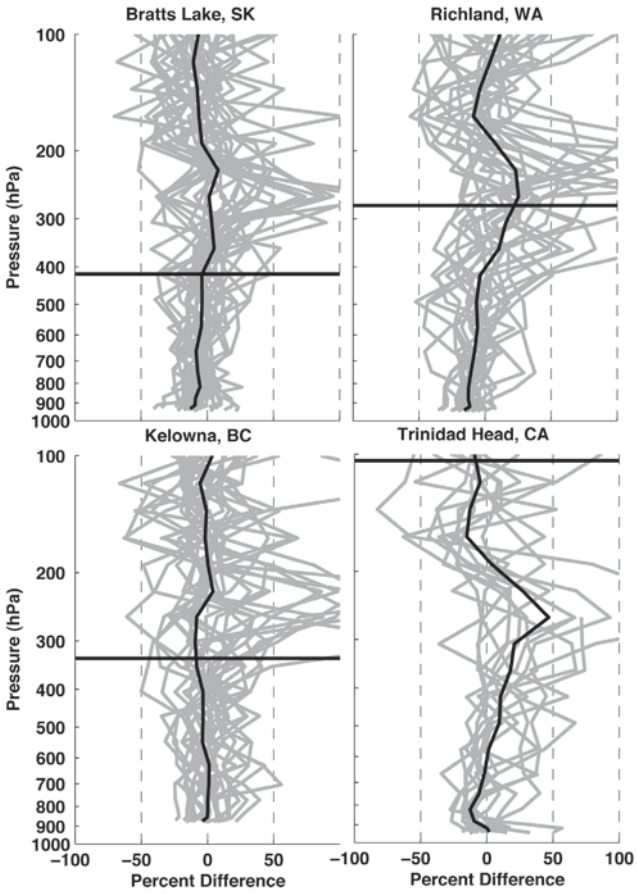

Figure 6. Percent differences between ASM and ozonesonde for each day of the study period were computed at each ASM pressure level by using average ozonesonde mixing ratios over each pressure level and are shown for each location in gray. The average percent differences over all days are shown by the black vertical profiles, while the horizontal bars represent the average dynamic tropopause heights, as defined by the TTOR product.

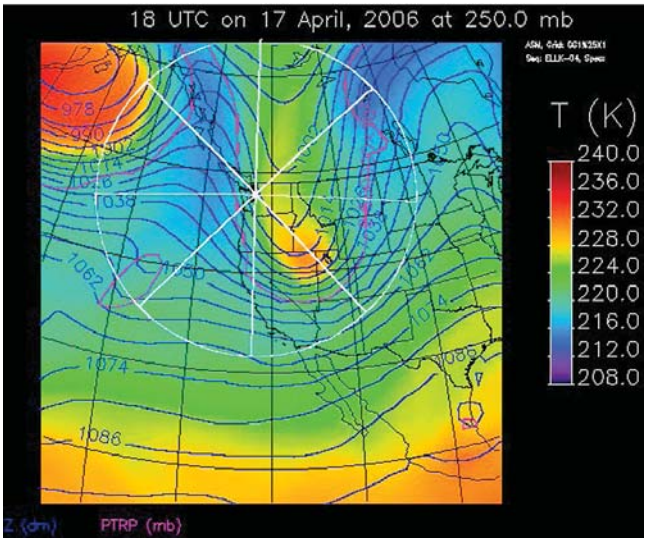

Figure 7. GEOS-4 atmospheric conditions at 250 HPa for Richland, Washington, at 1800 UT on 17 April 2006. Blue lines correspond to geopotential height in decameters, colors correspond to temperature, and the pink line represents the location where the tropopause is at 250 hPa. White lines radiate from Seattle where the NCAR C-130 aircraft was based during INTEX-B sampling. GEOS data are from http://croc/gsfc/nasa/gov/intex/IMAGES/CP.

tistics are representative of the performance of TTOR and ASM during the intense IONS-06 measurement period.

3.2. Satellite Comparisons

[22] The OMI instrument provides total ozone column measurements used for the TTOR and ASM calculations. The relationship between errors in ASM or TTOR tropospheric columns and errors in the OMI total column ozone can be seen for Bratt's Lake in Figure 4; note that other locations exhibited nearly the exact same behavior. Correlations for both data products are very low, with coefficients below 0.3 for both TTOR (n = 75) and ASM (n = 88). This suggests that local OMI values do not significantly contribute to the errors observed in these locations. ASM incorporates data from OMI measurements several days prior to the analysis day. Our present study has not examined the impact that those OMI measurements may have on the tropospheric column amounts.

3.3. Sonde and ASM Tropospheric Ozone Vertical Profiles

[23] Because the ASM product has twelve layers in the troposphere, we examine ozone profiles to obtain an in-depth look at ASM characteristics. An example comparing a typical ASM profile with the raw sonde data is seen in Figure 5.

[24] Percent differences at the middle of each ASM pressure level appear in Figure 6. For the comparisons, we compute mean ozonesonde-derived mixing ratios for each of the twelve ASM pressure levels. Individual gray lines show the percent difference between these ozonesonde mean mixing ratios and ASM mixing ratios for every day; black lines show average percent differences at each location.

[25] The profile comparisons indicate that the ASM biases generally fluctuate from negative in the lower troposphere to a positive peak around 250 hPa and again negative above 200 hPa. When column integration is performed, these positive and negative biases cancel, yielding a highly accurate ASM column product (recall that the average percent difference between ozonesondes and ASM is ~3%). This is not surprising because the observations used in the assimilation provide a constraint on the tropospheric column, but not the tropospheric profile below 215 hPa. The increased variability aloft may also be due to local dynamic uncertainty and complicated flow regimes. These possibilities are examined in case studies below.

[26] Figure 6 also provides support for the column integration height of 200 hPa [*Schoeberl et al.*, 2007]. The Trinidad Head, California, and Richland, Washington, locations have average dynamical tropopause heights above 300 hPa whereas Kelowna, British Columbia, and Bratt's Lake, Saskatchewan, have dynamical tropopause heights below 300 hPa (horizontal black lines in Figure 6 show average dynamical tropopause from TTOR product). At all four locations, ASM averages a positive bias between 300 and 200 hPa; this systematic bias was noted by *Stajner et al.* [2008]. Because the dynamical tropopause lies at a higher pressure than this region of positive bias at the higher-latitude locations but at lower pressure than the region of positive bias at lower-latitude locations, integration to dynamical tropopause could introduce a latitudinal bias.

3.4. Case Studies

[27] Section 3.3 shows that the ASM product usually exhibits high accuracy in tropospheric column ozone, but profile errors are quite variable. Because of this, we undertook two case studies in order to understand factors that may contribute to deficiencies in ASM tropospheric profiles. The first case examines the ASM-sonde agreement at Bratt's Lake, Saskatchewan, on 17 April 2006, when the location is under a strong upper level height gradient. The second case considers 21 April 2006 at Trinidad Head, California, when both ASM and TTOR are significantly different from the sonde measurement.

3.4.1. Bratt's Lake, Saskatchewan: 17 April 2006

[28] On 17 April 2006 a deep trough is near Bratt's Lake, Saskatchewan, and we observe a strong gradient in geopotential height over the launch site (Figure 7). Since a small difference in location may result in a significant difference in geopotential height, and since that difference may result in the inclusion of stratospheric air within the profile, it may be useful to consider all the ASM profiles in the vicinity of the sonde launch. To investigate this potential for variability, we consider the ASM profile that is co-located with the sonde launch, as well as ASM profiles from all adjacent pixels (Figure 8). On 17 April during the sonde's flight, winds were initially out of the north/northwest (http://croc.gsfc.nasa.gov/intexb/SONDES/profiles/O3SONDE_ bratt_20060417_pfl_gps.jpg). Near 800 hPa, winds have turned to the south, and remain generally southerly up above 100 hPa, so if the sonde were advected out of the pixel containing the launch, it would probably have entered the north or northeast pixel. Examination of

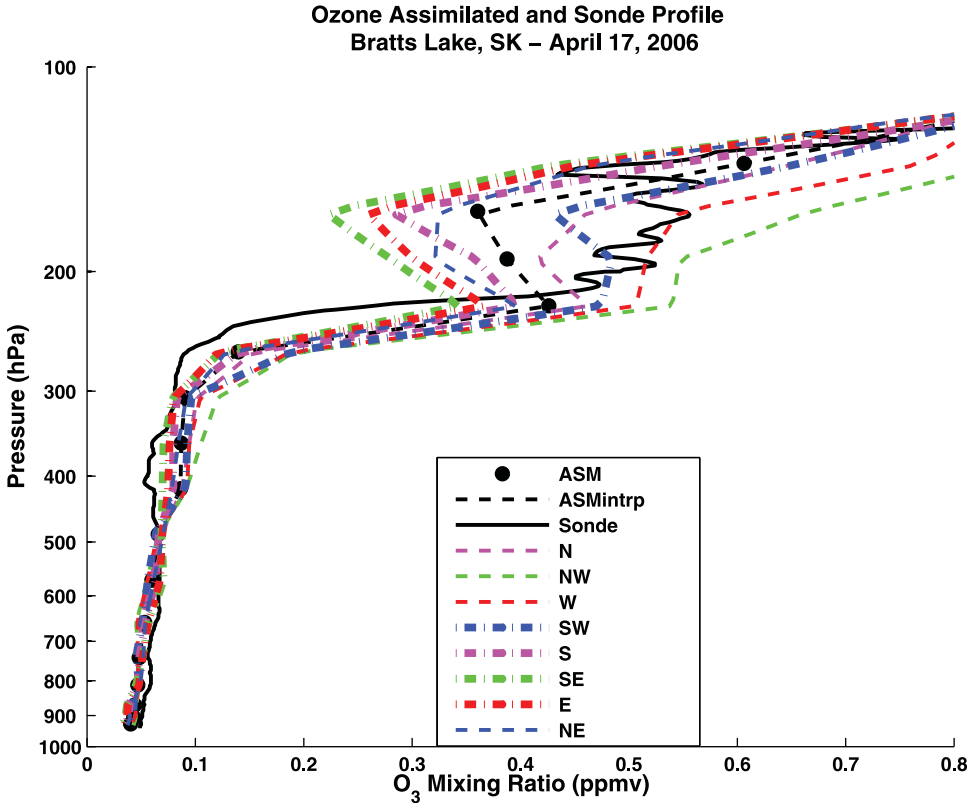

Figure 8. Profiles for Bratt's Lake on 17 April 2006. Solid black line shows ozonesonde profile, and dashed black line shows ASM retrieval from the pixel containing the launch site. All other lines come from adjacent pixels, as described in the legend.

the ASM profiles for this day shows that the modeled ozone profiles split near the UT/LS region (Figure 8). Near 200 hPa, the ASM pixel containing the ozonesonde launch, as well as pixels to the northeast, east, southeast, and south, have ozone mixing ratios 100 ppbv below that of the sondes, with the greatest discrepancy in the southeast. The other pixels exhibit more sonde-like behavior, and the northwest pixel is biased the highest of all of the profiles. The GEOS model output at 250 hPa (Figure 7) indicates strong geopotential height gradients from northwest to southeast; these are also evident at 100 hPa.

[29] Because both the gradient in geopotential height at 250 hPa is northwest to southeast and the gradient from higher to lower ozone is northwest to southeast, we infer that this is a case for which the dynamical conditions play the dominant role leading to the differences in ozone profiles. In section 3.4.2, however, it is seen that some discrepancies are not explained solely by synoptic conditions.

3.4.2. Trinidad Head, California: 21 April 2006

[30] On 21 April 2006, there is a significant discrepancy between the Trinidad Head ozonesonde and the ASM ozone retrievals (Figure 9b). Both the ASM and TTOR retrievals overestimate tropospheric column ozone by >50% above the ozonesonde surface to 200 hPa integration.

[31] GEOS meteorological fields show an upper level trough approaching the west coast of the United States, and Trinidad Head is near the center of that trough (Figure 10). An examination of the profile shows that, while there is a slight northeast/southwest progression in ozone mixing ratios in the upper troposphere, all ASM retrievals at and surrounding the pixel containing the Trinidad Head ozonesonde launch exhibit the same behavior. This suggests that local synoptic variability, or the passage of the sonde out of the ASM pixel, is not wholly responsible for the bias. OMI total column ozone is biased high (20 DU) compared with ozonesondes for this day, although correlations in section 3.4.1 suggest that in general, local OMI values do not drive the ASM or TTOR errors.

[32] We considered that the assimilation output time might have effected the ASM retrievals, since the assimilation data are output every 3 h. All our comparisons use ASM output at 2100 UTC, which is approximately the launch time of most sondes. On this day, the sonde was launched at 2028 UTC, so we also examined the assimilation outputs at 1800, 2100, and 0000 UTC to assess temporal influences on any observed discrepancies between satellites and sondes (Figure 9). We noted that there was little appreciable difference in the assimilation profiles for all three time steps.

[33] To assess uncertainty in advection we ran HYSPLIT back trajectories (R. R. Draxler and G. D. Rolph, HYSPLIT (HYbrid Single Particle Lagrangian Integrated Trajectory) Model, 2010, access via NOAA ARL READY Web site, http://ready.arl.noaa.gov/HYSPLIT.php; G. D. Rolph, Real-time Environmental Applications and Display sYstem (READY Web site, 2010, http://ready.arl.noaa.gov). Figures 11a and 11b shows 36 h back trajectories from 21 April 2100 UT initialized at 124.2°W and 41.8°N (red),

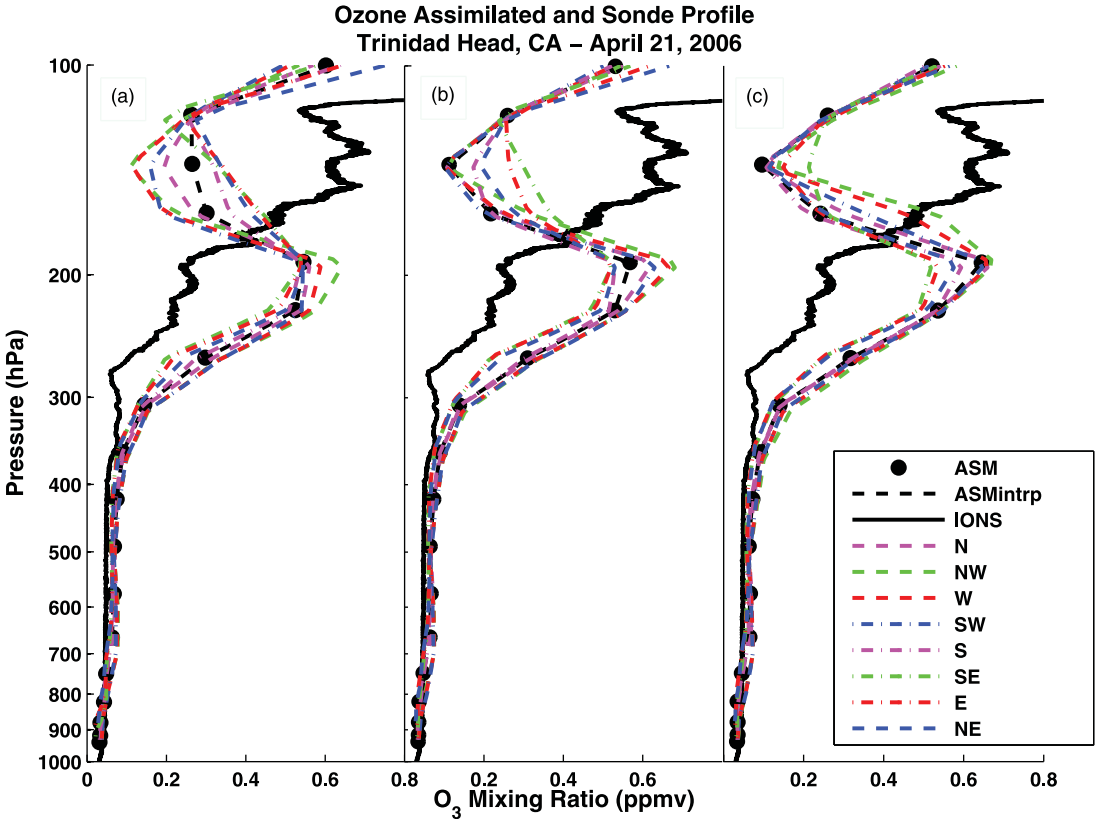

Figure 9. Progression of ASM retrievals for three output times. Black dashed line indicates the pixel that contains sonde launch, and other lines indicate adjacent pixels: (a) 1800 UT 21 April, (b) 2100 UT 21 April, and (c) 0000 UT 22 April.

40.8°N (blue) or 39.8°N (green). The blue trajectories correspond to Trinidad Head location. At the level of 11,000 m ASL, which is in the layer of strong overprediction in the assimilated profile, there is strong convergence of the flow and large uncertainty in the back trajectories. The 36 h back trajectory from the sonde location (blue) ends around 35°N with GDAS (Global Data Assimilation System) and around 50°N with EDAS (similar to GEOS-4 back trajectories, as in Figure 11c). Thus, due to strong convergence and uncertainty in the origin of the air mass that the sonde is sampling, even small offsets in the position or timing of atmospheric features could lead to large errors in the ozone fields. This is especially true given the variability in MLS measurements over the eastern Pacific Ocean the previous day (Figure 11d). Figure 12 lends credence to this hypothesis, since we observe that 10 degrees southwest of the sonde launch location, the elevated ozone in the upper troposphere is not seen in the ASM profile.

4. Conclusions

[34] Results from two recently developed methods of determining tropospheric ozone from Aura, a residual based technique and a data assimilation, were compared to ozone amounts (surface to 200 hPa) from ozonesonde profiles taken during IONS-06 (April/May 2006). The average bias for the Trajectory Enhanced Tropospheric Ozone Residual (TTOR) was −13.7 DU, and the average bias for the OMI/MLS Assimilation (ASM) was −1.33 DU, with correlation

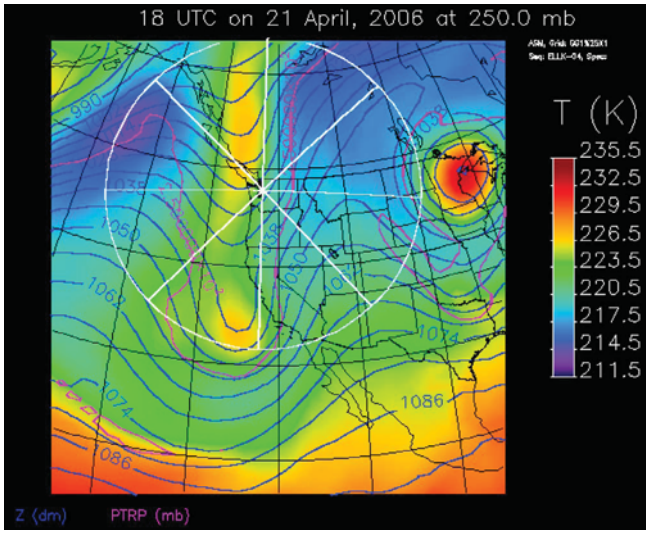

Figure 10. GEOS-4 atmospheric conditions at 250 hPa used to interpret data at Trinidad Head, California, on 21 April at 1800 UT. Blue lines correspond to geopotential height in decameters, colors correspond to temperature, and the pink line represents the location where the tropopause is at 250 hPa. GEOS data are from http://croc/gsfc/nasa/gov/intex/IMAGES/CP.

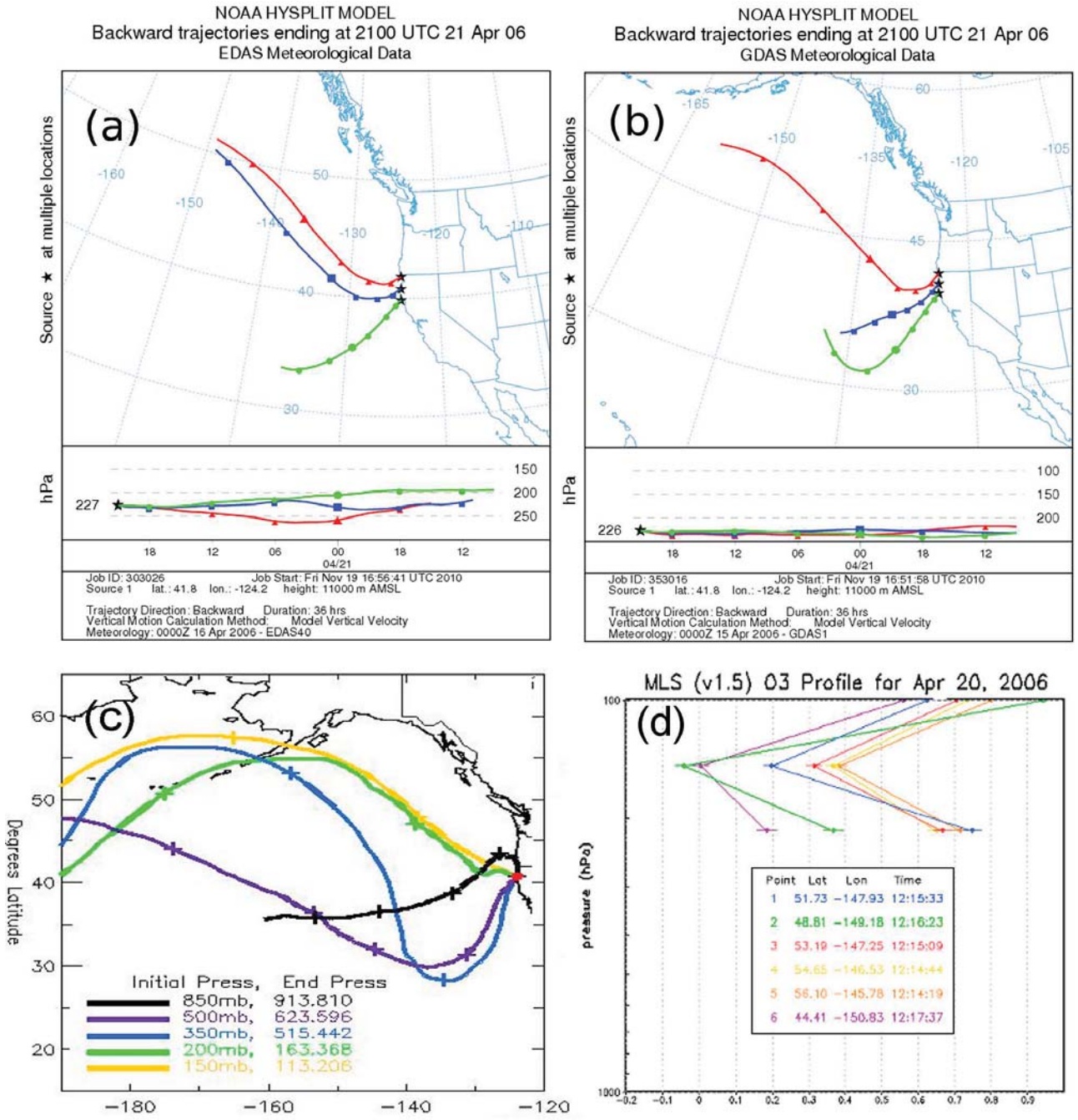

Figure 11. (a) HYSPLIT 36 h back trajectories initialized from 21 April 2010, using EDAS data. (b) Same as Figure 11a but with GDAS data. (c) Trajectories from GEOS-4 from 1800 UT on 21 April at five different levels (http://croc.gsfc.nasa.gov/intexb/SONDES/trajs/). (d) MLS measurements over the Pacific Ocean on 20 April 2006.

coefficients of 0.49 and 0.91, respectively. We observed that the low bias for the ASM product is partially due to systematic cancellation of errors in the lower and upper parts of the column, with some heights usually biased high and others biased low. Errors did not appear to be due to local OMI total ozone column retrieval errors, as correlation coefficients between total ozone and tropospheric ozone offsets with the sondes are below 0.3. However, the potential for errors in advection of information from MLS (for TTOR and ASM) and OMI (ASM) cannot be excluded.

[35] Because TTOR and ASM incorporate data from the same satellites and use the same model for transport, one might think that the two products would be more similar than they are. We noted that local total column estimations from OMI do not significantly affect the accuracy of either product. We suspect that the improved resolution of tropospheric transport processes in ASM, as well as its repre-

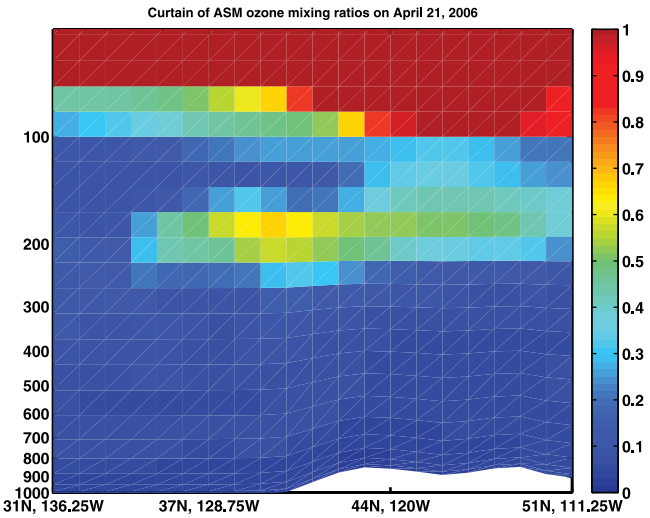

Figure 12. Curtain plot of ozone mixing ratios between 31°N, 136.5°W and 51°N, 111.25°W, roughly a line drawn southwest to northeast, centering on Trinidad Head (40.8°N 124.2°W). Colors correspond to ozone mixing ratio in ppm.

sentation of photochemistry and emissions, may account for the majority of the difference between ASM and TTOR.

[36] Two cases of sonde/ASM comparisons during this period were examined to better understand the effect of dynamics and transport on the ability of ASM to resolve tropospheric ozone. On 17 April 2006 at Bratt's Lake, Saskatchewan, the ASM profile in the pixel containing the sonde launch location does not capture the dynamical variations seen in the ozone profile, while adjacent locations in ASM have much better agreement with the sonde in the upper troposphere. Overestimates of the column at Trinidad Head, California, on 21 April by TTOR and ASM, and the disagreement between the profile shape of the sonde and ASM were probably related to uncertainty in the origin of the air masses in which the sonde was launched. These case studies illustrate some of the questions that remain about the performance of the ASM data product, as transport of ozone has the potential to play a significant role in any Aura-derived product which incorporates meteorological data.

[37] The springtime IONS-06 intensive campaign included launches in other locations, such as Valparaiso, Houston, Texas, and Mexico City [*Thompson et al.*, 2008]. These sites can be analyzed to better understand chemistry, transport, and ozone concentration relationships, including those in more polluted areas than the ones included here. Additionally, further research could incorporate statistical tools to characterize the performance of the ASM retrieval within different synoptic regimes.

[38] **Acknowledgments.** This work, based on the Masters Theses of D. C. Doughty and W. C. J. Hui, was sponsored by NASA's Aura Validation (M. J. Kurylo/K. W. Jucks) and Tropospheric Chemistry (B. G. Doddridge/J. H. Crawford/J. A. Al-Saadi) programs through grants. We are grateful to S. J. Oltmans, D. W. Tarasick, and J. C. Witte for the IONS ozonesonde data and to S. K. Miller for the GEOS meteorological data.

References

Balis, D., M. Kroon, M. Koukouli, E. Brinksma, G. Labow, J. Veefkind, and R. McPeters (2007), Validation of Ozone Monitoring Instrument total ozone column measurements using Brewer and Dobson spectrophotometer ground-based observations, *J. Geophys. Res.*, *112*, D24S46, doi:10.1029/2007JD008796.

Bloom, S., A. da Silva, and D. Dee (2005), Documentation and validation of the Goddard Earth Observing System (GEOS) Data Assimilation System - Version 4, *Tech. Rep. 26*, NASA Goddard Space Flight Cent., Greenbelt, Md.

Boyd, I., A. Parrish, L. Froidevaux, T. von Clarmann, E. Kyrölä, J. Russell, and J. Zawodny (2007), Ground-based microwave ozone radiometer measurements compared with Aura-MLS v2.2 and other instruments at two Network for Detection of Atmospheric Composition Change sites, *J. Geophys. Res.*, *112*, D24S33, doi:10.1029/2007JD008720.

Dougherty, K. M. (2008), The effect of ozonopause placement on tropospheric ozone budgets: An analysis of ozonesonde profiles from selected IONS-06 sites, Master's thesis, Pa. State Univ., University Park.

Douglass, A., C. Weaver, R. Rood, and L. Coy (1996), A three-dimensional simulation of the ozone annual cycle using winds from a data assimilation system, *J. Geophys. Res.*, *101*(D1), 1463–1474.

Fares, A., A. Goldstein, and F. Loreto (2010), Determinants of ozone fluxes and metrics for ozone risk assessment in plants, *J. Exp. Bot.*, *61*(3), 629–633, doi:10.1093/jxb/erp3366.

Felker, S. R., J. L. Moody, A. J. Wimmers, G. Osterman, and K. Bowman (2010), A Multi-sensor Upper Tropospheric Ozone Product (MUTOP) based on TES ozone and GOES water vapor: Derivation, *Atmos. Chem. Phys. Discuss.*, *10*, 30,055–30,087, doi:10.5194/acpd-10-30055-2010.

Fishman, J., C. Watson, J. Larsen, and J. Logan (1990), Distribution of tropospheric ozone determined from satellite data, *J. Geophys. Res.*, *95*(D4), 3599–3617, doi:10.1029/JD095iD04p03599.

Froidevaux, L., et al. (2008), Validation of Aura Microwave Limb Sounder stratospheric ozone measurements, *J. Geophys. Res.*, *113*, D15S20, doi:10.1029/2007JD008771.

Hudman, R. C., et al. (2007), Surface and lightning sources of nitrogen oxides over the United States: Magnitudes, chemical evolution, and outflow, *J. Geophys. Res.*, *112*, D12S05, doi:10.1029/2006JD007912.

Intergovernmental Panel on Climate Change (2007), *Climate Change 2007: The Physical Science Basis. Contribution of Working Group 1 to the Fourth Assessment Report of the Intergovernmental Panel on Climate Change*, edited by S. Solomon et al., Cambridge Univ. Press, New York.

Komhyr, W. (1969), Electrochemical concentration cells for gas analysis, *Ann. Geophys.*, *24*(1), 203–210.

Levelt, P. F., et al. (2006), The Ozone Monitoring Instrument, *IEEE Trans. Geosci. Remote Sens.*, *44*(5), 1093–1101, doi:10.1109/TGRS.2006.872333.

Liu, X., P. Bhartia, K. Chance, R. Spurr, and T. Kurosu (2010), Ozone profile retrievals from the Ozone Monitoring Instrumentozone profile retrievals from the Ozone Monitoring Instrument, *Atmos. Chem. Phys.*, *10*, 2521–2537, doi:10.5194/acp-10-2521-2010.

McPeters, R., M. Kroon, G. Labow, E. Brinksma, D. Balis, I. Petropavlovskikh, J. Veefkind, P. Bhartia, and P. Levelt (2008), Validation of the Aura Ozone Monitoring Instrument total column ozone product, *J. Geophys. Res.*, *113*, D15S14, doi:10.1029/2007JD008802.

Park, M., W. Randel, A. Gettelman, and S. Massie (2007), Transport above the Asian summer monsoon anticyclone inferred from Aura Microwave Limb Sounder tracers, *J. Geophys. Res.*, *112*, D16309, doi:10.1029/2006JD008294.

Pawson, S., I. Stajner, S. Kawa, H. Hayashi, W.-W. Tan, J. Nielson, Z. Zhu, L.-P. Chang, and N. Livesey (2007), Stratospheric transport using 6-h averaged winds from a data assimilation system, *J. Geophys. Res.*, *112*, D23103, doi:10.1029/2006JD007673.

Schoeberl, M. R., et al. (2007), A trajectory-based estimate of the tropospheric ozone column using the residual method, *J. Geophys. Res.*, *112*, D24S49, doi:10.1029/2007JD008773.

Singh, H., W. Brune, J. Crawford, F. Flocke, and D. Jacob (2009), Chemistry and transport of pollution over the Gulf of Mexico and the Pacific: Spring 2006 INTEX-B campaign overview and first results, *Atmos. Chem. Phys.*, *9*, doi:10.5194/acp-9-2301-2009.

Smit, H. G., et al. (2007), Assessment of the performance of ECC-ozonesondes under quasi-flight conditions in the environmental simulation chamber: Insights from the Juelich Ozone Sonde Intercomparison Experiment (JOSIE), *J. Geophys. Res.*, *112*, D19306, doi:10.1029/2006JD007308.

Stajner, I., et al. (2008), Assimilated ozone from EOS-Aura: Evaluation of the tropopause region and tropospheric columns, *J. Geophys. Res.*, *113*, D16S32, doi:10.1029/2007JD008863.

Thompson, A. M., et al. (2008), Tropospheric ozone sources and wave activity over Mexico City during Milagro/Intercontinental Transport

Experiment (INTEX-B) Ozonesonde Network Study, 2006 (IONS-06), *Atmos. Chem. Phys.*, *8*, 5113–5126, doi:10.5194/acp-8-5113-2008.

Thompson, A. M., S. J. Oltmans, P. von der Gathen, H. G. J. Smit, J. C. Witte, and D. W. Tarasick (2011), Strategic ozone sounding networks: Review of design and accomplishments, *Atmos. Environ.*, doi:10.1016/atmosenv.2010.05.002, in press.

Waters, J., et al. (2006), The Earth Observing System Microwave Limb Sounder (EOS MLS) on the Aura satellite, *IEEE Trans. Geosci. Remote Sens.*, *44*(5), 1075–1092, doi:10.1109/TGRS.2006.873771.

Yang, Q. D., D. Cunnold, H.-J. Wang, L. Froidevaux, H. Claude, J. Merrill, M. Newchurch, and S. Oltmans (2007), Midlatitude tropospheric ozone columns derived from the Aura Ozone Monitoring Instrument and Microwave Limb Sounder measurements, *J. Geophys. Res.*, *112*, D20305, doi:10.1029/2007JD008528.

Yang, Q. D., D. M. Cunnold, Y. Choi, Y. Wang, J. Nam, H.-J. Wang, L. Froidevaux, A. M. Thompson, and P. K. Bhartia (2010), A study of tropospheric ozone column enhancements over North America using satellite data and a global chemical transport model, *J. Geophys. Res.*, *115*, D08302, doi:10.1029/2009JD012616.

Yu, H., P. Wang, X. Zong, X. Li, and D. Lu (2010), Change of NO_2 column density over Beijing from satellite measurement during the Beijing 2008 Olympic Games, *Chin. Sci. Bull.*, *55*, 308–313, doi:10.1007/s11434-09-0375-0.

Zhang, J., D. J. Jacob, X. Liu, J. A. Logan, K. Chance, A. Eldering, and B. R. Bojkov (2010), Intercomparison methods for satellite measurements of atmospheric composition: application to tropospheric ozone from TES and OMI, *Atmos. Chem. Phys.*, *10*, 4725–4739, doi:10.5194/acp-10-4725-2010.

Zhang, Q., et al. (2009), Asian emissions in 2006 for the NASA INTEX-B campaign, *Atmos. Chem. Phys.*, *9* 5131–5153, doi:10.5194/acp-9-5131-2009.

Ziemke, J. R., S. Chandra, B. N. Duncan, L. Froidevaux, P. K. Bhartia, P. F. Levelt, and J. W. Waters (2006), Tropospheric ozone determined from Aura OMI and MLS: Evaluation of measurements and comparison with the Global Modeling Initiative's Chemical Transport Model, *J. Geophys. Res.*, *111*, D19303, doi:10.1029/2006JD007089.

D. C. Doughty and A. M. Thompson, Department of Meteorology, Pennsylvania State University, 503 Walker Bldg., University Park, PA 16802, USA. (dcd167@psu.edu; amt16@psu.edu)

W. C. J. Hui, Trinity Consultants, 12770 Merit Dr., Ste. 900, Dallas, TX 75251, USA. (jhui@trinityconsultants.com)

M. R. Schoeberl, Science and Technology Corporation, Hampton, VA 23666, USA. (mark.schoeberl@mac.com)

I. Stajner, Noblis Inc., 3150 Fairview Park Dr. S., MS F540, Falls Church, VA 22042-4519, USA. (Ivanka.Stajner@noblis.org)

K. Wargan, Global Modeling and Assimilation Office, NASA Goddard Space Flight Center, Greenbelt, MD 20771, USA. (krzysztof.wargan-1@nasa.gov)